Evaluation of 1/f Noise Characteristics for Si-Based Infrared Detection Materials

Hojun Ryu, Sein Kwon, Sanghoon Cheon, Seong Mok Cho, Woo Seok Yang, and Chang Auck Choi

Silicon antimony films are studied as resistors for uncooled microbolometers. We present the fabrication of silicon films and their alloy films using sputtering and plasma-enhanced chemical vapor deposition. The sputtered silicon antimony films show a low 1/*f* noise level compared to plasma-enhanced chemical vapor deposition (PECVD)-deposited amorphous silicon due to their very fine nanostructure. Material parameter *K* is controlled using the sputtering conditions to obtain a low 1/*f* noise. The calculation for specific detectivity assuming similar properties of silicon antimony and PECVD amorphous silicon shows that silicon antimony film demonstrates an outstanding value compared with PECVD Si film.

Keywords: Microbolometer, silicon antimony, resistor, noise.

I. Introduction

Infrared rays exist everywhere. Infrared rays were mentioned for the first time in a paper by Herschel in April of 1800 [1]. They affect many phenomena in our surroundings. Many studies have been conducted and many developments have been achieved on the use of infrared rays in various fields including military, medical, and industrial applications. Photon detection infrared sensors were developed in the 20th century. These detectors respond in the middle wavelength infrared range. Despite their high sensitivity, photon detectors require an expensive cryogenic cooling system. In order to respond in the mid-IR range, thermopile-, pyroelectric-, and bolometer-type detectors have competed in the commercial market. These days, the research trends regarding infrared sensors have shifted toward bolometric detection sensors. Among the many types of infrared detectors, uncooled microbolometers have been focused upon for their simple structure and outstanding performance. For a high-performance microbolometer, there has been a great deal of effort in seeking out bolometric materials [2]. Vanadium oxide is a well-known and widely used material for its high temperature coefficient of resistance (TCR) and low noise characteristics. However, it has the disadvantage that it is not suitable for a standard CMOS process. Studies on a-Ge:H or a-Si_xGe_{1-x}:H have been carried out in recent years [3]. Still, there has been no successful commercial use of these materials because of their process control problems. To achieve a high performance microbolometer, 1/*f* noise should be considered. Generally, materials having a high resistance have a high TCR and 1/*f* noise. Plasma-enhanced chemical vapor deposition (PECVD)-deposited amorphous silicon has been known to be a good candidate due to its thermal property and process compatibility. However, 1/*f*

Manuscript received Apr. 29, 2009; revised Sept. 14, 2009; accepted Oct. 9, 2009.

This work was supported by the IT R&D program of MIC/IITA, Rep. of Korea [2006-S054-01, Development of CMOS based MEMS processed multi-functional sensor for ubiquitous environment].

Hojun Ryu (phone: +82 42 860 1614, email: hjryu@etri.re.kr), Sanghoon Cheon (email: sh.cheon@etri.re.kr), Seong Mok Cho (email: smcho@etri.re.kr), Woo Seok Yang (email: wsyang68@etri.re.kr), and Chang Auck Choi (email: cachoi@etri.re.kr) are with the Convergence Components & Materials Research Laboratory, ETRI, Daejeon, Rep. of Korea.

Sein Kwon (email: sikwon@kaist.ac.kr) is with the Innovation Team for Advanced Process Integration, Hynix Semiconductor, Icheon, Rep. of Korea.

doi:10.4218/etrij.09.1209.0014

noise is a serious problem for obtaining high detectivity. According to previous studies, sputtered silicon shows lower 1/*f* noise than PECVD-deposited silicon film [4], [5]. Therefore, we have tried to find a new bolometric material for a microbolometer with high TCR, low 1/*f* noise level, and relatively low electrical resistance for the advantage of read-out integrated circuit (ROIC) fabrication. In this work, we have investigated the 1/*f* noise characteristics of new bolometric materials and compared them with the well-known PECVD-deposited amorphous silicon.

II. Experimental Procedure

Silicon antimony thin films were fabricated using a co-sputtering method for a new bolometric material. To regulate the element composition, we maintained independent bias power control. We deposited silicon nitride onto a silicon wafer for electrical insulation, patterned new materials for various shapes, and formed aluminum electrodes on the materials. In the case of amorphous silicon, the resistance is located within a range of a few mega-ohms to tens of mega-ohms. At the point of ROIC fabrication, the lower resistance is more effective, but the TCR is proportional to the logarithm of the resistivity. A compositional analysis was also carried out through Auger electron spectroscopy and was confirmed using Rutherford backscattering spectroscopy (RBS). The microstructure of silicon antimony thin films was analyzed using transmission electron microscopy. TCR values were measured using samples located on a thermo-electric cooler in order to maintain a uniform temperature control via an HP4156 I-V meter. We measured the 1/*f* noise characteristics using an SR 760 dynamic signal analyzer for various shape patterns. Figure 1 shows a schematic diagram of the 1/*f* noise measurement apparatus.

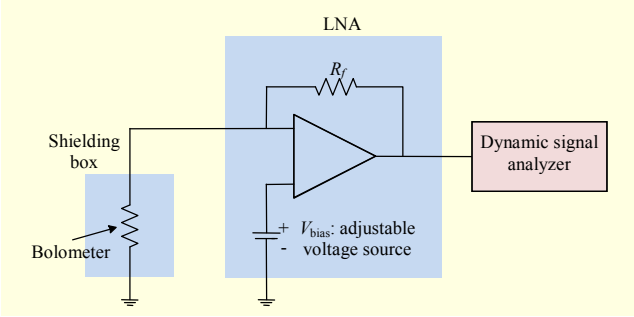

Fig. 1. Diagram of 1/*f* noise characteristic measurement system.

III. Results and Discussion

The optimum composition of a silicon antimony thin film having a high TCR is silicon alloy containing 40% antimony.

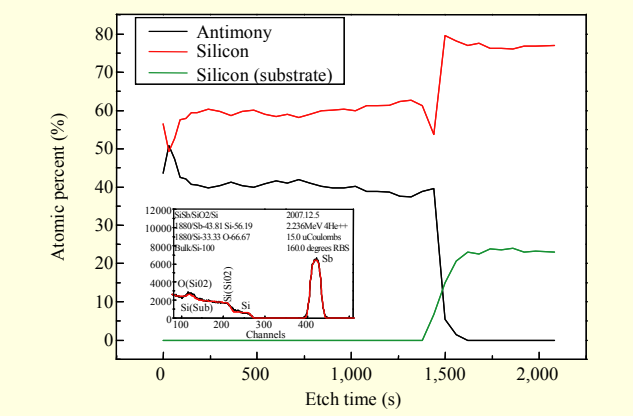

Fig. 2. Compositional analysis of $Si_{60}Sb_{40}$ film using AES and RBS.

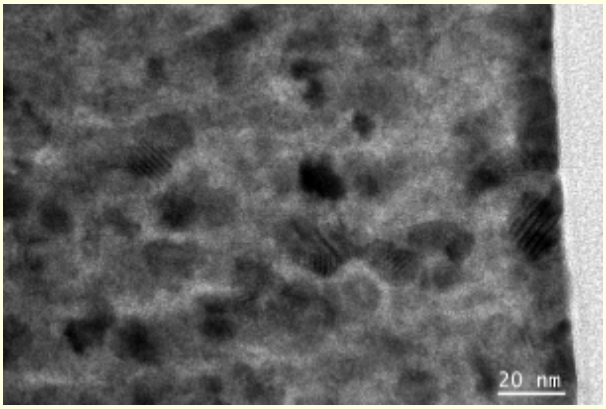

(a)

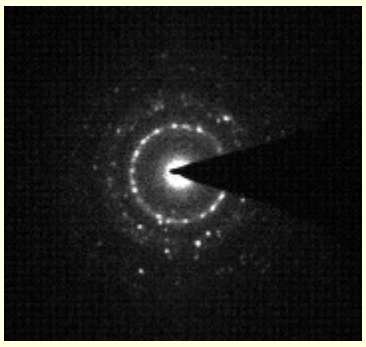

(b)

Fig. 3. TEM photos of $Si_{60}Sb_{40}$ film: (a) bright field image and (b) diffraction pattern.

As we mentioned previously, the composition was confirmed using RBS, which is shown in Fig. 2. The inset graph shows an RBS spectrum for $Si_{60}Sb_{40}$ film, and it matches well with the AES data. The origin of 1/*f* noise is still ambiguous; however, it is known that 1/*f* noise levels increase according to heterogeneity, impurities, and other film defects. Therefore, the microstructure of this silicon antimony film was investigated. Transmission electron microscopy images are shown in Fig. 3.

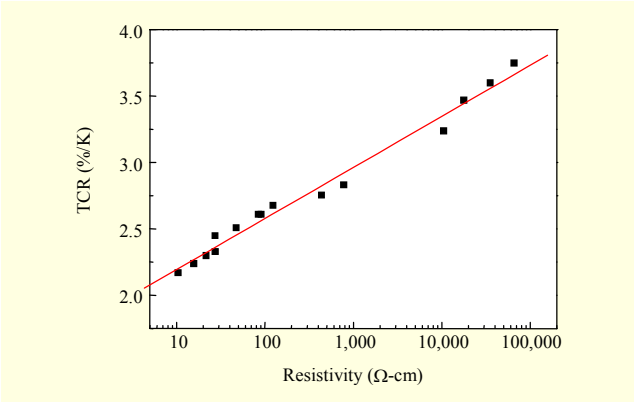

Fig. 4. TCR as a function of resistivity of silicon antimony alloy.

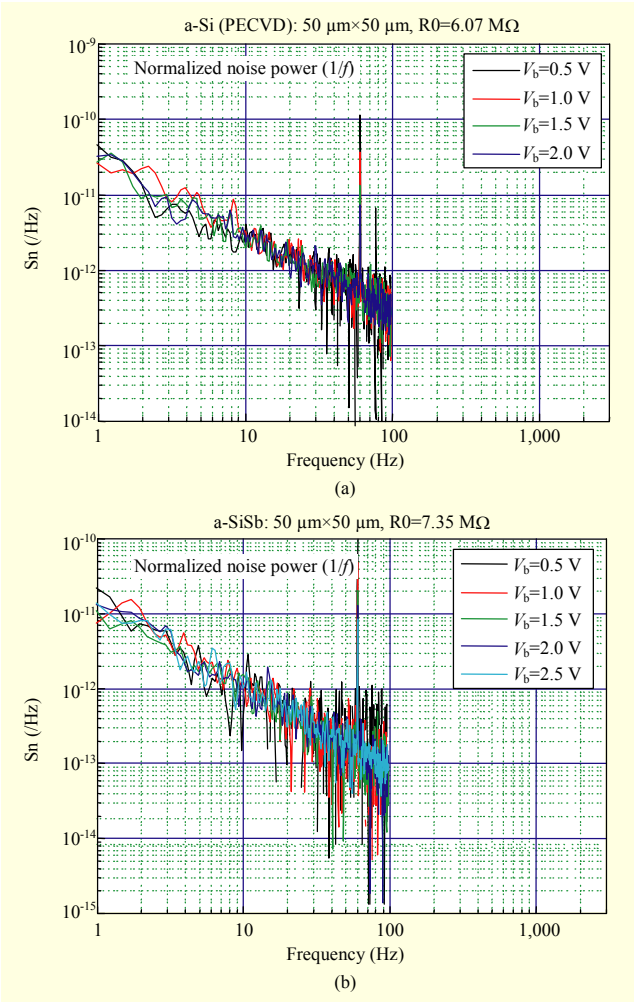

Fig. 5. The 1/*f* noise characteristics of (a) PECVD deposited silicon and (b) sputtered silicon antimony films.

In Fig. 3(a), a nano-size crystalline of a silicon antimony alloy is evenly distributed all over the film matrix. This can reduce the 1/*f* noise level of the new material. The size of the crystalline is under 20 nm, so in the x-ray diffraction patterns,

Table 1. Pattern size and resistivity of silicon antimony film for noise characterization.

	Width (μm)	Length (μm)	Area (μm^2)	Resistance factor
1	50	50,000	2,500,000	1,000
2		5,000	250,000	100
3		500	25,000	10
4		50	2,500	1
5		5	250	0.1
6	500	49,000	24,500,000	98
7		5,000	2,500,000	10
8		500	250,000	1
9		50	25,000	0.1
10	158	15,642	2,471,436	99
11		1,580	249,640	10
12		158	24,967	1
13		15.8	2,496	0.1
14	1,580	1,580	2,496,400	1
15		158	249,640	0.1

only the broad peaks are identified. In Fig. 3(b), rings in a diffraction pattern can be found. Therefore, silicon antimony thin film consists of finely formed crystalline. Figure 4 shows the TCR characteristics of deposited silicon antimony thin film. The measured TCR values are from 2%/K to 2.5%/K under the 100 Ω-cm range. Naturally, the TCR is proportional to the logarithm of resistivity, and materials having a high TCR value show high 1/*f* noise characteristics. Therefore, to obtain high figures of merit for a microbolometer, the high TCR and low 1/*f* noise need to be regulated. The 1/*f* noise characteristics were measured using an SR570 low-noise amplifier (LNA) and an SR760 dynamic signal analyzer as shown in Fig. 1.

Using a dynamic signal analyzer, the noise voltage was measured, and the current spectral density (S_{if}) was obtained from the value of the root mean square of 1/*f* noise voltage divided by the LNA gain. In (1), the relationship between the noise current spectra and 1/*f* noise parameter is given:

$$S_{if} = \frac{KI_b^2}{f^{\alpha}} \text{ (A}^2\text{/Hz)}, \quad (1)$$

where *K* is the 1/*f* noise parameter, and alpha is the power of *f*, the measuring frequency, which is usually close to 1. Using (1), the alpha of sputtered silicon antimony thin film is given as a range from 0.68 to 1.5 according to the frequency change when the bias current is set to 1 ampere for normalization of the compared data. To help explain the effects of the fabrication method of the film, we show the 1/*f* noise characteristics of sputtered silicon antimony and PECVD-deposited amorphous silicon films in Fig. 5. Using the same size area and similar

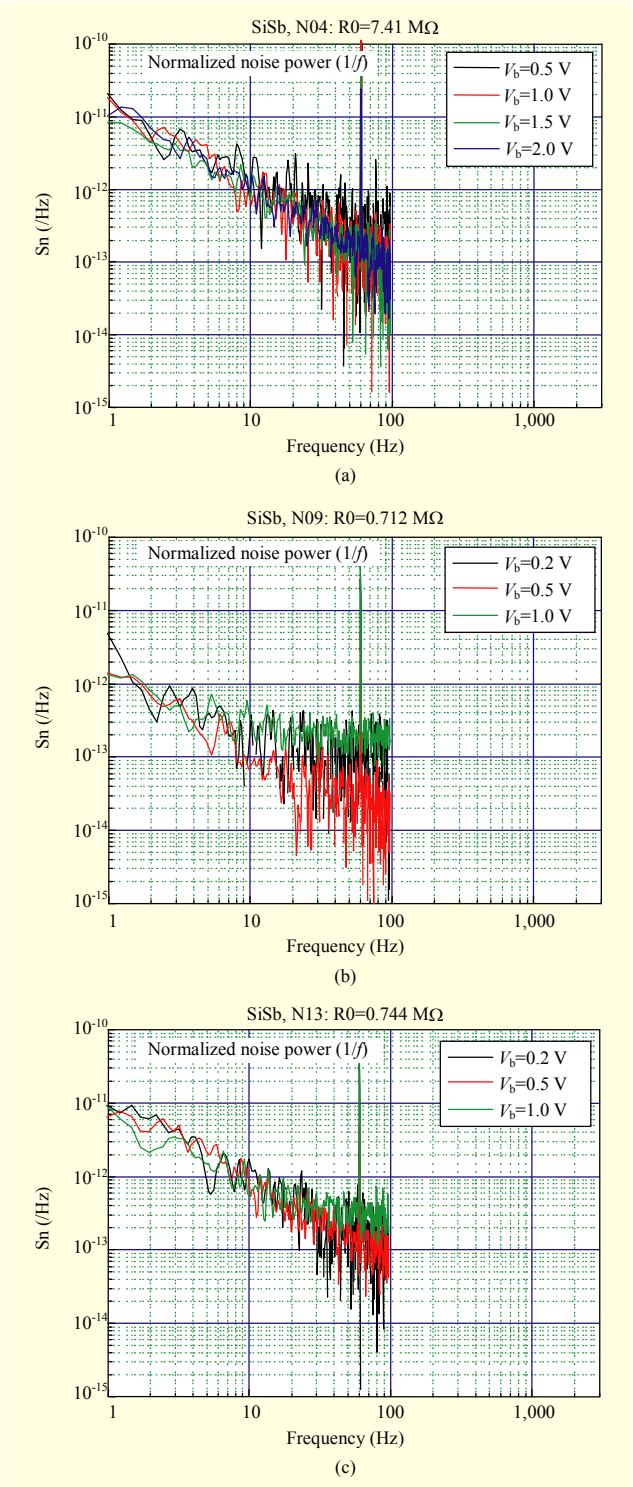

Fig. 6. The 1/*f* noise characteristics of sputtered silicon antimony film under various conditions.

resistivity, the 1/*f* noise level of silicon antimony is lower than that of PECVD-deposited amorphous silicon.

Furthermore, the resistance of silicon antimony is higher than that of PECVD amorphous silicon; therefore, the TCR of silicon antimony is higher than PECVD amorphous silicon because they have same resistance. The 1/*f* noise level can be compared with the 1/*f* noise parameter *K*, which is proportional to the total noise level. The total 1/*f* noise voltage is given by (2), where I_b is the bias current, *R* is the resistance, and BW indicates the bandwidth. Thus, the 1/*f* noise is also proportional to $K^{1/2}$. The related equation noise and material parameter *K* are also shown in (2). The calculated *K* value changes from 0.4×10^{-10} to 224.9×10^{-10} under a sputtering condition.

$$V_{1/f,\mathrm{rms}} = \sqrt{KI_b^2 R^2 \ln \mathrm{BW}} \quad (\mathrm{V}). \tag{2}$$

To compare the effect of volume change, we used sputtered silicon antimony films of various sizes as shown in Table 1. To control the measuring condition, the pixel resistance was changed with area. In this measurement, the resistance of a 50 micron by 50 micron pixel was set to 1, and the other size pixels were normalized by the resistance factor. Samples 4 and 13 were compared in terms of resistivity change. The effect of area change was also compared for samples 4 and 9 under the same resistivity. Comparing the noise levels in Figs. 6(a) and (c), there is no effect of resistivity change. When the total noise is the same as parameter *K*, and the resistivities have an inverse proprotion relationship, a resitivity effect is not considered to exist. According to the nature of 1/*f* noise, there is no volume change effect.

There is only 1/*f* noise increment with a volume change effect in Figs. 6(b) and (c). As samples with well-defined areas, they could have the same resistivity. In this case, the area defined by the etching process is not perfect. Hence, the resistivity change causes a noise level difference between the samples.

The most important figure of merit of a microbolometer is detectivity for real applications. In many cases, the areas of detectors vary with their design rules. To compare the performance of the detectors without the area factor, the specific detectivity, which is considered an area factor, was used. For the compared films, which were fabricated using different deposition methods and adopted for the resistor layer of a microbolometer, the specific detectivity was calculated. In

Table 2. Microbolometer parameters for detectivity calculation.

Factor	Value
Emissivity (ε)	0.8
TCR (α)	2.24 to 2.73 (%/K)
Pixel area (μm^2)	44 × 46
Bandwidth	5,000 Hz
Starting time	0.0001 Hz
Thermal conductance (*g*)	5×10^{-8} (W/K)

the calculations, their common environmental conditions were set equally. The compared parameters of the films were set as shown in Table 2. The specific detectivity for devices with normalized area and bandwidth is given by

$$D^* = \frac{R_v\sqrt{A_d \cdot \mathrm{BW}}}{V_{n,\mathrm{rms}}} = \frac{V_{\mathrm{bias}}\alpha\varepsilon}{g}\frac{\sqrt{A_d \cdot \mathrm{BW}}}{V_{n,\mathrm{rms}}}. \quad (3)$$

IV. Conclusion

The calculated results of detectivity are shown in Table 3 for PECVD deposited amorphous silicon and sputtered silicon antimony films having a similar TCR. The total noise voltage including 1/*f* noise of the PECVD-deposited film is 20 times higher than that of the sputtered film. Therefore, the detectivity of a device with sputtered silicon antimony as a resistor layer is much better than the detectivity when PECVD-deposited film is used. The new bolometric material for microbolometer application was fabricated using silicon and antimony. The microstructure of the sputtered silicon antimony film has evenly-distributed nano-sized crystalline, which produces good 1/*f* noise characteristics. Comparing the calculated detectivity when using the developed film as a resistor layer, the sputtered silicon antimony shows a better performance for microbolometer applications.

Table 3. Calculated detectivity of sputtered silicon antimony and PECVD-deposited silicon films.

	$V_{n,\mathrm{rms}}$ (μV)	TCR (%/K)	D^* (cmH$^{1/2}$/W)
PECVD	1656.8	-2.2	2.82E8
Sputter	89.2	-2.24	5.32E9

References

[1] W. Herschel, "Experiments on the Refrangibility of the Invisible Rays of the Sun," *Phil. Trans. Roy. Soc. of London*, vol. 90, 1800, pp. 284-292.

[2] P.L. Richards, "Bolometers for Infrared and Millimeter Waves," *J. Appl. Phys.*, vol. 76, no. 1, 1994, pp. 1-24.

[3] M. Garcia et al., "IR Bolometers Based on Amorphous Silicon Germanium Alloys," *J. Non-Cryst. Solids.*, vol. 338-340, 2004, pp. 744-748.

[4] M.H. Unewisse et al., "Growth and Properties of Semiconductor Bolometers for Infrared Detection," *Proc. SPIE*, vol. 2554, 1995, pp. 43-54.

[5] P.W. Kruse and D.D. Skatrud, *Uncooled Infrared Imaging Arrays and Systems*, Academic Press, San Diego, 1997.

Hojun Ryu received the BS, MS, and PhD degrees in material science and engineering from Seoul National University, Seoul, in 1986, 1993, and 1998, respectively. From August 1999 to February 2001, he worked as a postdoctoral research fellow at the University of Texas at Austin. He has been with ETRI as a senior research staff member since 2001. He has researched in the fields of MEMS devices and nanostructures fabrication of functional materials. Currently, he is involved in several research projects including the development of a microbolometer and tire pressure monitoring systems. He was promoted to the manager of the Future Core Technology Team in July 2009. He is an editorial committee member of the Electronic Materials Letters.

Sein Kwon received the BS and MS degrees in electrical engineering and computer science from KAIST, Daejeon, in 2006 and 2008, respectively. He worked on the development of a sputtered amorphous silicon-antimony alloy for bolometer resistors. In 2008, after receiving his MS degree, he joined Hynix Semiconductor, Rep. of Korea, where he is involved in the development of the sub-30 nm DRAM.

Sanghoon Cheon received the BS, MS, and PhD degrees in electrical engineering and computer science from KAIST, Daejeon, in 1993, 1995, and 2001, respectively. In 2001, he joined Knowledge-on Inc., Rep. of Korea, where he worked in the 6-inch InGaP/GaAs HBT foundry service business, as well as working on large signal modeling for microwave devices, and the development of power amplifiers for WCDMA system until 2005. In 2006, he moved to ETRI, Daejeon, where he has been involved in the development of the microbolometer for infrared focal plane arrays. He is interested in uncooled infrared imaging arrays and systems.

Seong Mok Cho received the BS, MS, and PhD degrees in materials engineering from Pohang University of Science and Technology (POSTECH), Korea, in 1992, 1994, and 2001, respectively. From February 1994 to January 1996, he worked as a research engineer with the semiconductor division of Samsung Electronics. He has been with ETRI as a senior member of engineering staff since 2001. His current research interests are sensor technologies, such as infrared image sensors and electronic noses.

Woo Seok Yang received the BS, MS, and PhD degrees in materials science and engineering from Pohang University of Science and Technology, Pohang, Korea, in 1991, 1993, and 1998, respectively. From 1998 to 2001, he worked on FeRAM and DRAM at Hynix Semiconductor Inc. He has been with ETRI since 2001. His recent research interests are in the fields of physical MEMS devices and advanced functional materials.

Chang Auck Choi received his MS and PhD degrees in electronic engineering from Kyungpook National University, Daegu, Korea, in 1988 and 1999, respectively. Since 1980, he has been working for ETRI in the area of developing micro-electro-mechanical-system (MEMS) devices and advanced semiconductor process technology. He is currently the project manager of MEMS sensor technology development. His research interests are physical sensors and integrated MEMS sensor and process.